Analyst

Accepted Manuscript

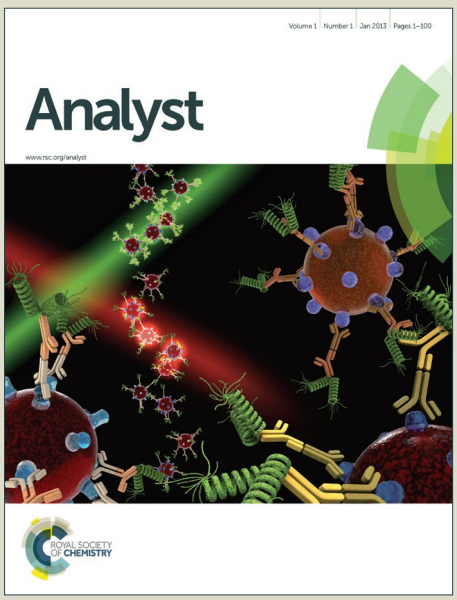

ROYAL SOCIETY OF CHEMISTRY

www.rsc.org/analyst

Analyst

RSCPublishing

ARTICLE

Monitoring electron and proton diffusion flux through three-dimensional, paper-based, variable biofilm and liquid media layers

Cite this: DOI: 10.1039/x0xx00000x

Received 00th January 2012,
Accepted 00th January 2012

DOI: 10.1039/x0xx00000x

www.rsc.org/

Gihoon Choi, and Seokheun Choi*

The goal of this work is to pursue analytical approaches that elucidate electron and proton diffusion inside the *Shewanella oneidensis* biofilm and bulk liquid, which will inevitably promote the translation of Microbial Fuel Cell (MFC) technology for renewable, "green energy" solutions that are in demand to sustain the world's ever-increasing energy demands and to mitigate the depletion of current resources. This study provides a novel strategy for monitoring electron/proton fluxes in 3-D multi-laminate structures of paper as a scaffold to support *S. oneidensis* biofilms and bulk media liquid. Multiple layers of paper containing bacterial cells and/or media are stacked to form a layered 3-D model of the overall biofilm/bulk liquid construct. Mass transport of electrons and protons into this 3-D system can be quantified along with the exploration of microbial energy production. Assembly of a 3D paper stack can be modular and allows us to control the thickness of the overall biofilm/bulk liquid construct with the different diffusion distances of the electrons/protons through the stack. By measuring the current generated from the 3-D stack, the electron and proton diffusivity through biofilms were quantitatively investigated. We found that (i) the diffusion length of the electrons/protons in the *S. oneidensis* biofilm/bulk liquid is a determinant factor for the MFC performance, (ii) the electron transfer through the endogenous mediators of *S. oneidensis* can be a more critical factor to limit the current/power generation of the MFCs than the proton transfer in the MFC system and (iii) the thicker biofilm allows higher and longer current generation but requires more time to reach a peak current value and increases the total energy loss of the MFC system.

1. Introduction

Microbial fuel cells (MFCs) have attracted considerable attention in the last decade, especially after a significant breakthrough was made through the discovery of mediator-less bacterial species.[1,2] These bacteria are operationally stable and significantly improve the power generation of the MFC by several orders of magnitude.[3-5] However, the ability to harness the potential of the advanced MFC technology is still restrained due to our lack of an in-depth understanding of the key mechanisms underlying electron harvesting from electroactive microbial biofilms, and other fundamental factors responsible for determining MFCs' electricity-generating capabilities.[6,7] In particular, monitoring the electron/proton fluxes and quantifying the temporal and spatial gradients of nutrients/redox mediators inside MFC systems – critical processes that control electron transfer between the microorganisms and an electrode and ensuing power output – is challenging, and the techniques to accomplish these measurements are limited.[8-10] Moreover, constrained mass transport of the ions/metabolites will produce the heterogeneities in the biofilm that are leading factors in the degradation of power/current output of the MFC which can be better elucidated by monitoring the spatial characteristics of electron/proton transport through the biofilm matrix.[9,11,12] Such heterogeneities may account for why biofilm thickness is one of the critical variables for the transport of the electron/proton/nutrients/redox mediators since their diffusions could be hindered by the biofilm matrix.[13-15] Renslow et al., for example, measured the *in-situ* effective diffusivity of water inside *Shewanella oneidensis* biofilms and found that thick biofilms showed a relative effective diffusivity as low as 50%.[9] Moreover, the pH inside the biofilm is expected to decrease during diffusion; metabolism generates protons along with electrons, and while electrons move toward the electrode surface, protons move towards the bulk solution.[8]

Bioelectronics & Microsystems Laboratory, Department of Electrical & Computer Engineering, State University of New York-Binghamton, Binghamton, NY 13902, USA
**Corresponding Author. Email: sechoi@binghamton.edu*

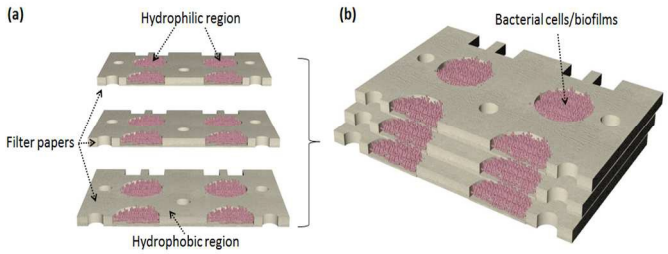

Figure 1. Conceptual illustration of the 3D stackable multi-laminate structure of papers as a scaffold to support bacterial cells and media. (a) Multiple layers of paper containing bacterial cells were stacked to form (b) a layered 3-D model of the overall biofilm construct.

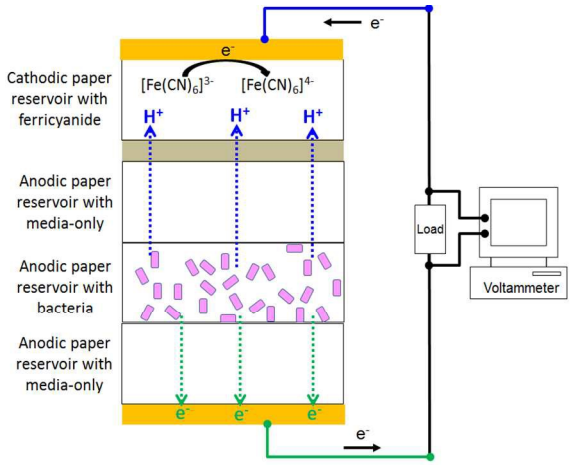

Figure 2. Schematic diagram of the proof-of-concept device. Electricity measured from the 3D paper stack will vary according to the number of anodic paper reservoirs containing bacteria and/or media, controlling the thickness of bacterial biofilm and proton/electron traveling distances.

Understanding the microscale development of pH inside biofilms will allow us to distinguish the critical role that pH plays in the electron transfer. At the same time, the electron flux inside the biofilm is expected to cause a distribution of potential inside the biofilm—one that is dependent on the resistance across endogenous shuttling mediators, conductive nanowires, or both.[8]

To date, many innovative and novel approaches have been proposed. MEMS micro-needles have been utilized as an alternative method for quantifying critical parameters inside biofilms,[16] but their invasive technique uses ferricyanide, which destroys the biofilm and thus does not allow for time series measurements.[10] The recently-developed pulsed-field gradient Nuclear Magnetic Resonance (NMR) technique also suffers from inherently low sensitivity due to its low energies.[10] It requires careful optimization to decrease measurement times and concentration detection thresholds.[17] NMR systems are bulky, heavy and expensive, further limiting their capability and accessibility. Moreover, none of the techniques control biofilm thickness. Therefore, real-time, *in-situ,* non-invasive techniques with controllability of biofilm thickness will allow for better-characterized correlations between bacterial electrogenic behavior and biofilm formation. In particular, knowledge of electron/proton diffusion in living biofilms/bulk liquid will be critical for engineering systems to manipulate bacterial biofilms for other purposes, such as the penetration of antibiotics into biofilms of pathogenic bacteria, heavy metal immobilization in environmental biofilms, and the penetration of organic molecules and oxygen into biofilm for wastewater treatment.[10]

In this work, we provided a new analytical technique that allows us to control the thickness of the overall biofilm construct, modulating diffusion of electrons/protons through the biofilm and bulk liquid (Fig 1). Multiple layers of filter paper containing bacterial cells/biofilms were stacked to form a layered 3-D model of the overall biofilm construction, and mass transport of electrons/protons into this 3-D system were quantified along with the better interpretation of the bacterial electron transfer mechanisms. Simply stacking media-only containing layers with bacteria-containing layers can adjust the diffusion length of protons/electrons generated from microbial metabolism in biofilm (Fig 2). This new sensing platform will also promote understanding of the temporal and spatial gradients of nutrients/redox mediators through the biofilm, which is another limiting factor for biofilm growth and metabolism, and which affects how long these fuel cells can practically generate energy.

2. Materials and methods

2.1 MFC principle

In MFCs, electrons are generated from chemical bonds with the aid of microbial metabolism.[18, 19] The produced electrons are then transported to the anode surfaces and flow through an external load while the anode is connected to cathode. The flow of the electrons develops a current and a potential drop through the load. The proton transfer through the proton exchange membrane between the anode and cathode is necessary to maintain MFC electroneutrality. Therefore, electron and proton transfers inside the MFC system play a profound role in determining the MFC performance.

The microorganisms transfer electrons produced via metabolism across the cell membrane to an external electrode; this process is called extracellualr electron transfer (EET).[20, 21] Three EET mechanisms have been proposed: (i) direct electron transfer, where the bacterial cells attach physically to the anode and transfer electrons, (ii) shuttle transfer, where electrons are transferred to the anode via electron mediators, and (iii) nanowire transfer, where a solid conductive wire is synthesized and utilized for electron transfer. In this work, we selected *Shewanella oneidensis* as a model microorganism. Recent reports show that electron transfer via chemical shuttles play an important role in *Shewanella oneidensis*, with ~ 90% of EET occurring through this mechanism.[22, 23] Therefore, *Shewanella oneidensis* can be an appropriate model species to investigate electron/proton fluxes in the controlled, multi-layered, 3-D biofilm and bulk liquid.

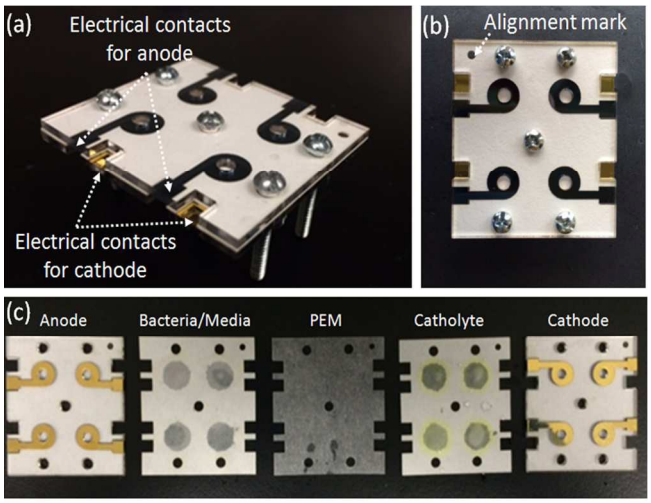

Figure 3. (a) & (b) Photo-images of the assembled device and (c) individual layers including paper reservoirs after loading the anolyte and catholyte. Hydrophilic sample regions are made by hydrophobic wax boundaries.

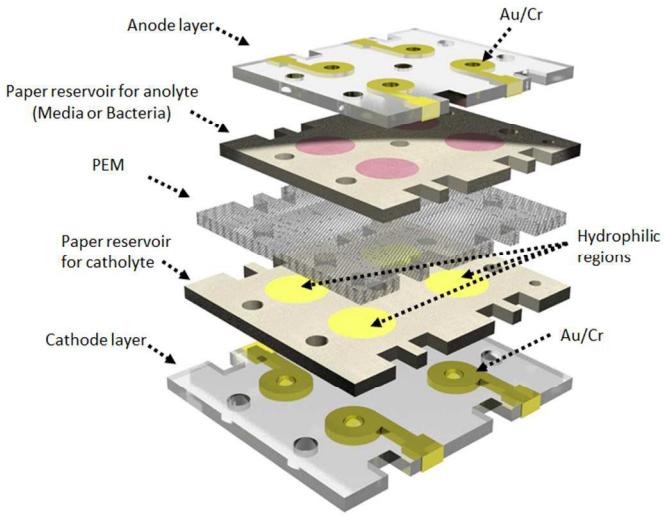

Figure 4. Schematic diagram of individual layers of the device. The device consists of five functional layers: anode/cathode layer, anodic/cathodic paper reservoir, and paper proton exchange membrane. Anolyte and catholyte were trapped in the hydrophilic regions on paper. Several anodic paper reservoir layers were stacked to control the proton/electron travel distance in the MFC system.

2.2 Device fabrication

Fig. 3 describes our assembled 3-D paper based microbial sensing platform. The sensor included four spatially distinct wells of the sensor array. We leveraged the techniques recently demonstrated for paper-based MFC devices,[21, 24-26] and paper-based 3-D culture systems.[27-29] Each MFC stack contained five functional layers: anode/cathode layers (Au/Cr on 1.6mm-thick polymethyl methacrylate (PMMA)), anodic/cathodic paper reservoir layers (Whatman #1, ~180µm thick), and a paper-based proton exchange membrane (PEM) (Reynolds Parchment Paper, ~50µm thick) (Fig 3 & Fig 4). Each layer was micro-patterned using laser micromachining (Universal Laser System VLS 3.5). The anode and cathode layers were prepared by depositing 200nm gold on PMMA substrates with 20 nm chrome as the adhesion layer. The layers had metal pads (10 mm diameter) with through-holes in the center for use when we needed to directly introduce anolyte/catholyte into the anodic/cathodic paper reservoirs. Paper reservoirs featuring a hydrophilic chamber with hydrophobic wax boundaries were microfabricated by heat pressing commercially available wax paper onto a filter paper.[24] This paper-based platform can be easily directed toward the development of a much higher throughput array.

2.3 Anolyte and catholyte

Wild-type *Shewanella oneidensis* MR-1 was aerobically cultivated in L-broth medium (10.0 g tryptone, 5.0 g yeast extract and 5.0 g NaCl per unit liter) at room temperature. Growth was monitored by measurement of the optical density at 600 nm (OD_{600}) and culture we used reached an OD_{600} of 0.5. 20 µl inoculum for bacteria-containing layer or L-broth medium for media-only layer were loaded on four independent wells on the patterned paper with hydrophobic barriers. The paper layers with bacterial cells were further cultured in their media for four hours to form a biofilm in paper matrix. The catholyte was 50 mM ferricyanide in a 100 mM phosphate buffer in which the pH was adjusted to 7.5 ± 0.2 with 0.1 M NaOH. At the cathode, ferricyanide, $[Fe(CN)_6]^{3-}$, captures the electrons (Eq. (1)) and the cycle is completed (Fig 2).

$$[Fe(CN)_6]^{3-} + e^- \rightarrow [Fe(CN)_6]^{4-} \quad (1)$$

2.4 Assembly

The paper-based reservoirs allowed for rapid adsorption of bacteria-containing liquid or media-only solution.[21, 24-26] This adsorption immediately promoted bacteria cell attachment to the paper fibres to form a 3D biofilm-like structure, reducing the time traditional culture systems require to accumulate and acclimate bacteria on the surface. The paper reservoir layers also held the media and catholyte for the MFC electrochemical reactions during the extended period of time. Different stack configurations were prepared with different sets of bacteria-containing and media-only containing layers. Each layer of a stack configuration was carefully aligned and vertically stacked with the other functional layers such as anodic/cathodic layers and the PEM. The fabricated stack formed a MFC system from which the current generation could be measured.

2.5 Measurement setup

The potential differences between the anode and the cathode were measured through a data acquisition system (National instrument, USB-6212). The data were recorded every 20 sec via a customized LabView interface (Fig. 2). An external load resistor (4.7 kΩ) was connected between the each MFC unit's anode and cathode to enable current production through the resistor by Ohm's law (I = V/R).

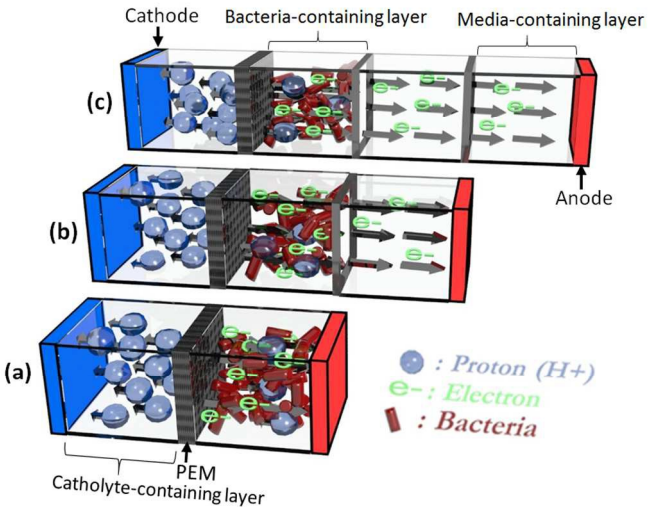

Figure 5. Devices with different electron traveling distances in the MFC. Electron travel distance was modulated as a limiting factor of MFC performance. When a media-only containing layer is placed between the bacteria-containing layer and anode, the electron traveling distance in the system increases; (a) no media layer, (b) one media layer and (c) two media layers between the bacterial layer and anode. The (c) produced the longest electron traveling distance.

3. Results and discussion

To demonstrate our proof-of-concept, we developed a simple paper-based MFC stack. Multiple paper layers containing bacterial cells formed a layered 3D biofilm construct which controlled the biofilm thickness while the liquid media layers produced different experimental sets with different electron/proton traveling distances. Our hypothesis was that (i) electron and proton traveling distances were controllable according to the location a media-only layer was positioned and the number of the layers included. In addition, (ii) their effects on MFC performances were investigated by measuring the microbial current generation. Finally, (iii) their electricity generations could be also monitored across different biofilm thicknesses. Distinct spatial wells of the sensor provided repeated experiments four times, generating error bars in the results.

3.1 Electron traveling distance

When a media-only containing paper layer is placed between the bacteria-containing layer and anode, the electron traveling distance increases in the MFC, affecting its electrical current generation. Fig 5 shows the experimental approach about how the electron traveling distance can be modulated as the sole limiting factor for MFC performance. We prepared three paper-based devices to allow for different electron traveling distances: Fig 5a produced the shortest electron traveling distance while Fig 5c generated the longest one with two additional media layers. The single cathodic reservoir layer containing 50 mM potassium ferricyanide enabled the devices to produce the same proton traveling distance.

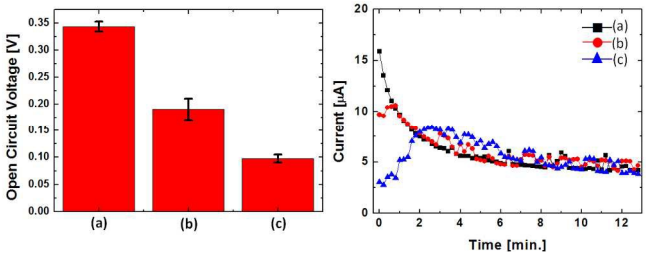

Figure 6. Open Circuit Voltages (OCVs) and current profiles measured from the devices shown in Fig 5, describing correlation between electron transport and MFC performance. The experiment provided three different electron diffusion lengths (length from the bacteria-containing layer to the anode:((a) < (b) < (c)).

The open circuit voltages (OCVs) of the devices were measured for the first 3 minutes to compare the initial device performances. The cell electromotive force (emf) is theoretically defined as the potential difference between the anode and cathode, which ideally corresponds to the OCV.[30] However, the OCV is substantially lower than the cell emf due to the energy loss of the MFC system. Although it is not easy to obtain the theoretical cell emf in this work due to the overall complexity of the LB media we used, Fig 6 clearly shows that the OCV significantly decreases by ~30% with an additional media-containing layer between the bacteria-containing layer and anode, indicating that the bulk liquid formed between the anode and biofilm increases the total energy loss of the system. The MFCs can reduce the total energy loss of the MFC by decreasing the bulk liquid thickness between the anode and biofilm, ultimately enhancing the total cell voltage (E_{cell}) and thus, the power (P) as well. The total cell voltage calculated as:[10, 21]

$$E_{cell} = OCV - I \cdot R_{int} \quad (2)$$

,where E_{cell} is the cell voltage at a current I and R_{int} is the internal resistance. The total power of the system can be calculated as:

$$P = I \cdot E_{cell} \quad (3)$$

After measuring the OCVs under no-load conditions, the 4.7 kΩ resistors were connected between anodes and cathodes to enable current production. The voltage differences under the resistor were recorded to obtain the current profile through the resistor (Fig 6). The device with the shortest electron traveling distance, without any media-containing layer instantly generated the maximum current immediately after the resistor connection, which then gradually decreased. This instant current generation from the device agrees well with our previous paper-based MFCs.[21, 24-26] This is primarily due to the rapid microbial metabolic electron transfer in the paper matrix. Immediate power generation of *Shewanella oneidensis* was

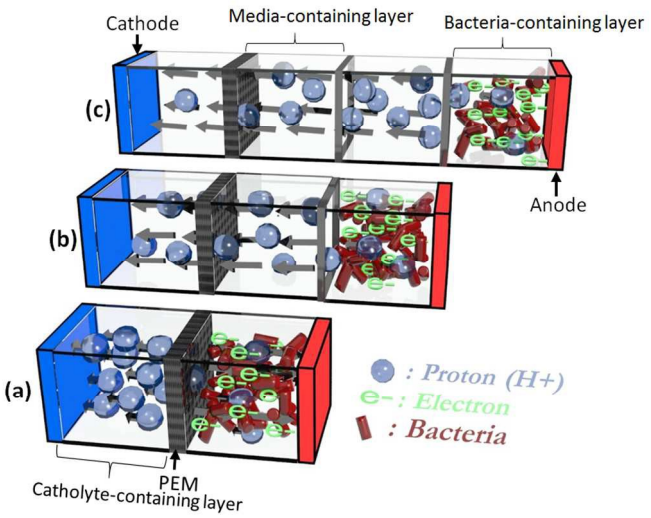

Figure 7. Devices with different proton traveling distances in the MFC. Proton travel distance was modulated as a limiting factor of MFC performance. When a media-only containing layer is placed between the PEM and bacteria-containing layer, the proton traveling distance in the system increases; (a) no media layer, (b) one media layer and (c) two media layers between the PEM and bacterial layer. The (c) produced the longest proton traveling distance.

achieved through the shuttling transfer mechanism as we discussed in the previous section. However, as an additional media-containing layer was introduced between the bacterial layer and the anode, the device required more time to reach a peak current value, which was lower than that of the device without the media layer. This is because (i) the electrons via shuttle compounds should travel more distance with the additional media layer and (ii) the total internal resistance (R_{int}) increases as well. The internal resistance can be described by equation (4):[31]

$$R_{int} = R_a + R_m + R_c + R_e \quad (4)$$

where R_a, R_m, R_c, and R_e are anodic, membrane, cathodic, and electrolyte resistance, respectively. While R_a, R_m and R_c are consistent with all devices in Fig 5, R_e is the only variable as the media layer is added. R_e can be calculated by:

$$R_e = l / (A \cdot K) \quad (5)$$

where l is electrode distance (cm) and A is the cross-sectional area (cm^2) through which ionic conduction occurs, and K is the specific conductivity ($\Omega^{-1} \cdot cm^{-1}$) of the electrolyte. The thickness of the paper layer containing the media was 0.018 cm, the conductivity of the medium was 0.010 $\Omega^{-1} \cdot cm^{-1}$,[32] and the cross sectional area of each region containing the media was 0.785 cm^2. We then computed R_e as 2.29Ω with one media-containing layer.

The maximum current value decreased by ~29% with an additional media layer, and produced 8μA with the two layers. Fig 6 shows that the electron traveling distance is a significant

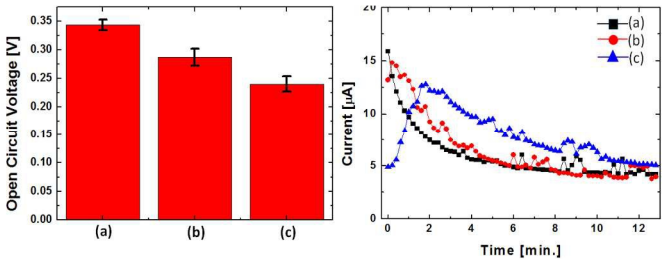

Figure 8. Open Circuit Voltages (OCVs) and current profiles measured from the devices shown in Fig 7, describing correlation between proton transport and MFC performance. The experiment provided three different proton diffusion lengths (length from the bacteria-containing layer to the cathode: ((a) < (b) < (c)).

factor in limiting the power generation of the MFCs. Based on equation (3), the total power for the MFC considerably decreases due to the reduction of both the OCV and current as electron traveling distance increases. The power considerably dropped by ~56% as the electron traveling distance increased with one media layer.

3.2 Proton traveling distance

When a media-only containing layer is positioned between the PEM and bacterial layer, the proton traveling distance increases. Fig 7 shows the experimental approach about how the proton traveling distance in the MFC system can be controlled as a limiting factor for MFC performance. We prepared three paper-based devices to allow for different proton traveling distances: Fig 7a produced the shortest proton traveling distance while Fig 7c generated the longest one with two additional media layers. The single bacterial layer positioned between the anode and media layer enabled the devices to produce the same electron traveling distance. The protons released by microbial metabolism travel through all the media layers and the PEM towards the cathode. Fig 8 shows the OCVs and currents measured from the devices with different proton traveling distances. The OCVs of the system decreases by ~14% with the media-containing layer between the PEM and the bacteria-containing layer, indicating that the bulk liquid formed between the PEM and biofilm increases the total energy loss of the system.

The maximum current value decreased by ~12% with an additional media layer, and generated 13 μA with the two layers. The introduction of the additional media layer delayed the time for the device to reach the maximum current value. The total power of the MFC decreased by 17% as the proton traveling distance increased with a single media layer, indicating that the proton traveling distance also negatively affects the MFC power generation.

Based on our experiments, however, electron transfer is a much more critical factor to determine MFC performance than proton transfer, especially in the case where the bacteria have the shuttling transfer mechanism for EET.

3.3 Biofilm thickness

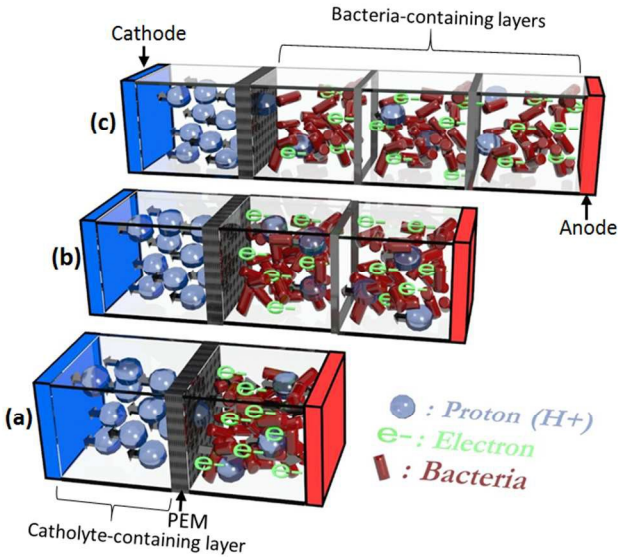

Figure 9. Devices with different biofilm thicknesses in the MFC. Bacteria-containing paper layers were introduced between the anode and PEM; (a) one bacterial layer, (b) two bacterial layers and (c) three bacterial layers.

The electrical behaviours were also monitored across different biofilm thicknesses (Fig 9). Stacking of cell-containing constructs allowed us to provide different bacterial biofilm thicknesses for better understanding of the effect that the biofilm thickness has on MFC performances. By introducing the additional layers containing bacterial cells, electrons/protons will have larger traveling distances and may decrease the power/current generation as shown in Fig 6 & 8. However, we need to consider the increased amounts of the electrons/protons produced from additional bacterial cells, which may inversely increase their electricity generation. As shown in Fig 10, the OCV decreases with the additional paper layer due to the total energy loss as in the previous experiments on electron/proton traveling distances. However, the OCV with two additional layers was higher than that with one additional layer, indicating that the total energy loss in MFCs can be reduced with thicker biofilms. It should be noted that the maximum current generation increases with the additional cell-containing layers and reaches the highest value of ~20 μA with the two layers. Moreover, the thicker biofilm allowed longer current generation, increasing the total energy density of the MFC system.

3.4 Diffusion coefficient of electrons and protons

The diffusion of the electrons and protons in MFCs can be calculated by Fick's diffusion law. For three-dimensional semi-infinite linear diffusion with one flow direction, the diffusivity (D) can be obtained by:[9]

$$x = \sqrt{2Dt} \qquad (6)$$

,where x is the diffusion layer thickness and t is the diffusion time. Fig 11a shows the time required for each device

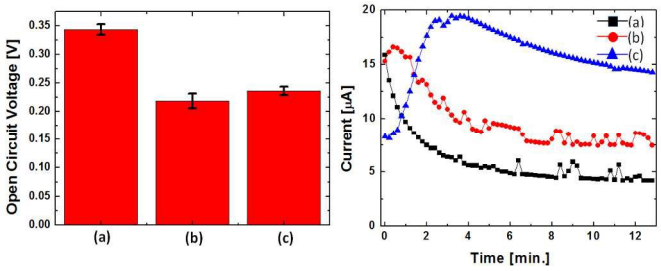

Figure 10. Open Circuit Voltages (OCVs) and current profiles measured from the devices shown in Fig 9, describing correlation between biofilm thickness and MFC performance. The experiment provided three different biofilm thicknesses ((a) < (b) < (c)).

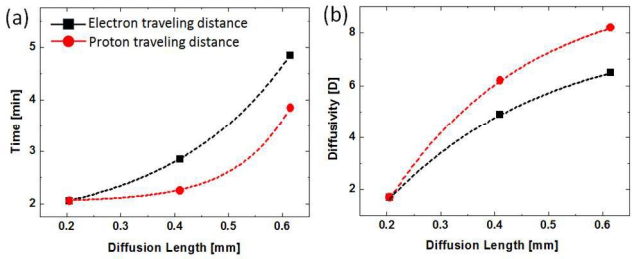

Figure 11. (a) The time required for the device to reach the maximum current value versus diffusion lengths for electrons/protons in media-containing layers. (b) the diffusivity (given in 10^{-6} $cm^2 \cdot s^{-1}$) versus the diffusion lengths

configuration to reach the maximum current value versus the diffusion lengths with the paper reservoir layers inserted, while Fig 11b shows the calculated diffusivities (D) versus the diffusion lengths according to the experimental setups shown in Fig 5 and Fig 7. The protons traveling in the media-containing layers required a shorter time to generate the peak current value than the electron's, producing a higher diffusivity, 8.2×10^{-6} $cm^2 \cdot s^{-1}$. This number is one order of the magnitude lower than the proton diffusivity reported from the previous study.[33] This is probably because the protons traveling in this work can be interfered with 3-D paper matrix. However, our approach provided a sensing platform that can control the biofilm thickness in three dimensions and the mass transport of electrons/protons. For the last experimental setup shown in Fig 9, the diffusivities cannot be obtained because it was difficult to distinguish between electron and proton diffusion.

4. Conclusion

We introduced a novel strategy for exploring the diffusions of electrons/protons in electrogenic bacterial biofilms and/or in bulk liquid and investigated their effects on MFC performances. The paper-based multi-laminate structural platform provided a controllable and three-dimensional biofilm and bulk liquid construct in the MFC system. By measuring the current generated from different MFC stack configurations, the diffusion of the electrons/protons were quantitatively investigated. These efforts were demonstrated by creating spatially distinct wells in the MFC array that provided four

simultaneous measurements. We found that the electron flux is more critical than the proton flux in the *Shewanella oneidensis* biofilms and depend on the shuttling transfer mechanism for electricity generation. Diffusivity of the electrons and protons in the MFC system were also calculated. This work is part of a global effort to understand how the electron/proton fluxes develop in biofilm and bulk media, how EET occurs in biofilms and how these phenomena can be applied for beneficial purposes. This work will also provide a novel approach to investigate the nutrients and other electrochemical gradients in living biofilms and/or bulk media and will contribute to an in-depth understanding of EET of electrogenic bacterial.

Acknowledgement

This work is supported by NSF (ECCS #1503462).

References

1 Z. Du, H. Li, T. Gu, *Biotechnology Advances*, 2007, **25**, 464-482.
2 K. Rabaey, W. Verstraete, *Trends in Biotechnology*, 2005, **23**, 291-298.
3 B.E. Logan, *Appl. Microbiol. Biotechnol.*, 2010, **85**, 1665-1671.
4 B.E. Rittmann, *Biotechnology and Bioengineering*, 2008, **100**, 203-212.
5 V.B. Oliveira, M. Simoes, L.F. Melo, A.M.F.R. Pinto,, *Biochemical Engineering Journal,* 2013, **73**, 53-64.
6 J. Babauta, R. Renslow, Z. Lewandowski, H. Beyenal, *Biofouling*, 2013, **28**, 789-812.
7 A.P. Borole, G. Reguera, B. Ringeisen, Z. Wang, Y. Feng, B.H. Kim, *Energy Environ. Sci.,*, 2011, **4**, 4813-4834.
8 H. Beyenal, J.T. Babauta, *Biochem. Soc. Trans.*, 2012, **40**, 1315-1318.
9 R.S. Renslow, P.D. Majors, J.S. McLean, J.K. Fredrickson, B. Ahmed, H. Beyenal, *Biotechnol. Bioeng.*, 2010, **106**, 928-937.
10 R.S. Renslow, J.T. Babauta, P.D. Majors, H. Beyenal, *Energy Environ. Sci.,*, 2013, **6**, 595-607.
11 P.S. Stewart, *Journal of Bacteriology*, 2003, **185**, 1485-1491.
12 P.S. Stewart, M.J. Franklin, *Nat. Rev. Microbiol.*, 2008, **6**, 199-210.
13 S. Choi, J. Chae, *Sensors and Acuators: A. Physical*, 2013, **195**, 206-212.
14 S.T. Read, P. Dutta, P.L. Bond, J. Keller, K. Rabaey, *BMC Microbiology*, 2010, **10**, 98.
15 L. Zhang, X. Zhu, J. Li, Q. Liao, D. Ye, *Journal of Power Sources*, 2011, **196**, 6029-6035.
16 W.H. Lee, W. Choi, X. Guo, W.R. Heineman, P.L. Bishop, *Key Engineering Materials*, 2012, **521**, 113-139.
17 K. Vafai, *CRC Press, Taylor & Francis Group*, 2010, August 24 (ISBN 9781420065411)
18 D.R. Lovely, *Annual review of microbiology*, 2012, **66**, 391-409.
19 S. Choi, *Biosensors and Bioelectronics*, 2015, **69**, 8-25.
20 C.I. Torres, A.K. Marcus, H. Lee, P. Parameswarn, R. Krajmalnik-Brown, B.E. Rittmann, *FEMS Microbiol Rev.,* 2010, **34**, 3-17.
21 A. Fraiwan, H. Lee and S. Choi, *IEEE Sensors Journal*, 2014, **14**, 3385-3390.
22 D. Coursolle, D.B. Baron, D.R. Bond, J.A. Gralnick, *Journal of Bacteriology*, 2010, **192**, 467-474.
23. N.J. Kotloski, J.A. Gralnick, *mBio*, 2013, **4**, e00553-12.
24 T.H. Nguyen, A. Fraiwan, S. Choi, *Biosensors and Bioelectronics*, 2014, **54**, 640-649.
25 A. Fraiwan, S. Mukherjee, S. Sundermier, H.-S. Lee, S. Choi, *Biosensors and Bioelectronics*, 2013, **49**, 410-414.
26 A. Fraiwan, S. Choi, *Physical Chemistry Chemical Physics*, 2014, **16**, 26288-26293.
27 B. Mosadegh, B.E. Dabriri, M. Lockett, R. Derda, P. Campbell, K.K. Parker, G.M. Whitesides, *Adv. Healthcare Mater.,* 2014, **3**, 1036-1043.
28 B. Mosadegh, M.R. Lockett, K.T. Minn, K.A. Simon, K. Gilbert, S. Hillier, D. Newsome, H. Li, A.B. Hall, D.M. Boucher, B.K. Eustace, G.M. Whitesides, *Biomaterials*, 2015, **52**, 262-271.
29 M.C. Sapp, H.J. Fares, A.C. Estrada, K.J. Grande-Allen, *Acta Biomaterialia*, 2015, **13**, 199-206.
30 B.E. Logan, B. Hamelers, R. Rozendal, U. Schroder, J. Keller, S. Freguia, P. Aelterman, W. Verstraete, K. Rabaey, *Environmental Science & Technology*, 2006, **40**, 5181-5192.
31 S. Choi, H.-S. Lee, Y. Yang, P. Parameswaran, C.I. Torres, B.E. Rittmann, J. Chae, *Lab on a Chip*, 2011, **11**, 1110-1117.
32 Y. Son, J. Phue, L.B. Trinh, S. Lee, J. Shiloach, *Microbial Cell Factories*, 2011, **10**, 52.
33 C.I. Torres, A.K. Marcus, B.E. Rittmann, *Biotechnol. Bioeng.*, 2008, **100**, 872-881.